Hindawi
Shock and Vibration
Volume 2022, Article ID 3532331, 21 pages
https://doi.org/10.1155/2022/3532331

Research Article

Influence of Abutment Stiffness and Strength on the Seismic Response of Horizontally Curved RC Bridges in Comparison with Equivalent Straight Bridges at Different Seismic Intensity Levels

Khashayar Heydarpour and Payam Tehrani

Department of Civil and Environmental Engineering, Amirkabir University of Technology, Tehran, Iran

Correspondence should be addressed to Payam Tehrani; payam.tehrani@aut.ac.ir

Received 15 April 2022; Revised 24 October 2022; Accepted 31 October 2022; Published 25 November 2022

Academic Editor: Mohammad Amin Hariri-Ardebili

Seismic design codes have imposed some limitations on the maximum subtended angle of curved bridges and allow engineers to analyze and design them using an equivalent straight bridge. This paper investigates these limitations and evaluates the AASHTO code recommendations regarding the prediction of the seismic responses of curved bridges using an equivalent straight bridge for bridges with different abutment properties at different seismic hazard levels. In this regard, the seismic responses of 21 horizontally curved and straight RC four-span bridges with different abutment types are investigated. In 7 bridge models, soil-abutment-bridge interaction is neglected, while in the rest of the bridge models, the seat-type abutments with the participation of the nonlinear backfill soil, gap, and abutment piles are used in structural modeling. First, nonlinear static (pushover) analyses are carried out to evaluate the overall behavior of the bridges with different abutment configurations in the two perpendicular principal directions. Subsequently, nonlinear time history analyses are performed to predict the seismic response of bridge elements, including column drifts and deck displacements at the place of the abutments in the radial and tangential directions at different seismic intensity levels, including the design basis earthquake (DBE) and maximum credible earthquake (MCE) excitation levels. In addition, the actual maximum displacements of the components of the bridges (i.e., the total absolute displacements) were also predicted and evaluated for different cases. It was found that the abutment properties and boundary conditions had a significant effect on the seismic response assessment of curved bridges compared to straight bridges, while such parameters are not currently considered by the design codes. The results also indicated that by increasing the seismic intensity level, more limitations should be imposed on the use of the equivalent straight bridges.

1. Introduction

Horizontally curved bridges have become popular in congested urban areas, where a strong emphasis on aesthetic and environmentally friendly structural design exists [1, 2]. Curved bridges with subtended angles greater than certain limits are considered irregular bridges in bridge design codes [3, 4]. It has been shown in the past that irregular bridges are more vulnerable to seismic excitations compared to regular bridges [5–11]. Experience with past earthquakes proved that this class of bridges is more vulnerable to seismic excitations than that of bridges with straight and skewed typologies. The collapse of curved reinforced concrete (RC) bridges during the 1971 San Fernando earthquake in California [12, 13], failure of the newly built Baihua Bridge [14–17], and other simply supported continuous girder bridges [18] due to the 2008 Wenchuan earthquake in China are a few examples. Bridge design codes allow designers to use an equivalent straight bridge in lieu of a horizontally curved bridge to simplify its computer modeling, analysis, and design [3, 4]. However, the use of such equivalent bridges is limited to curved bridges with certain limits on their subtended angle and regularity. Irregular geometry and nonuniform mass distribution in curved bridges lead to an excessive in-plane rotation of the superstructure compared to an equivalent straight bridge [19]. Unseating of the

superstructure is one of the primary collapse modes of horizontally curved bridges, exacerbated by the increased in-plane rotation of the superstructure [20]. Although the scope of this paper is to evaluate the seismic performance of RC box-girder bridges, a few pieces of literature have been reviewed in association with steel girder bridges to highlight the adverse effects of curvature and evaluate the vulnerability of curved bridges to earthquake excitations. According to a probabilistic-based study conducted by AmiriHormozaki et al. [21], as the central angle in horizontally curved steel I-girder bridges increases, the demand for column ductility and bearing deformations at the abutment in both directions increases up to 44%. Other parametric studies regarding the seismic response of curved steel I-girder bridges unanimously confirm that the radius of curvature had the most significant impact on the seismic performance of this class of bridges [22–24]. Minavand and Ashtiany [25] conducted a parametric study based on the model of Sadr Elevated Bridge, located in the northeast of Tehran, with a horizontally curved RC box-girder typology. They concluded that increasing the curvature of the deck leads to an increase in seismic displacement demand of piers, shear force, and bending moment demands of the deck and piers. According to further seismic fragility-based probabilistic evaluations of horizontally curved multicolumn and single-column bent RC box-girder bridges, curvature is identified to be an important parameter that adversely influences the fragility of multiframe bridges [26]. Although horizontal curvature significantly affects fragilities for some components, it has a relatively minimal influence on the system fragility [27]. Shirazi et al. [28] developed horizontally curved RC box-girder bridge models based on current seismic design considerations incorporated with modern details adopted by Caltrans. They deduced that columns were the most vulnerable components, while the modern seismic details successfully protected abutment piles from damage during large earthquakes. It is also found that horizontal curvature increases bridge vulnerability irrespective of the design era and height range, and its adverse effects on seismic performance are more prominent for bridges with single pier bents [29, 30].

The influence of soil-structure interaction (SSI) on the dynamic responses of bridges is non-negligible. According to a study conducted by Tang et al., based on the shear wave velocity of soil, the SSI effect both increases and decreases the dynamic responses of large-span bridges [31]. Abutment walls were traditionally designed to withstand active and passive Earth pressures. However, seismic excitation induces higher inertial loads than anticipated passive Earth pressure conditions [32]. Under certain design considerations, abutments also participate in the earthquake-resisting system (ERS) of the bridge [33, 34]. Abutment modeling reduces seismic responses and column ductility demands up to 80% [8]. The seat-type abutment is commonly used for long-span, highly skewed, or highly curved bridges to avoid large or unbalanced stresses in the superstructure and embankment backfill soil under thermal loads [20]. Column high ductility demand and deck unseating are two major modes of failure due to seismic excitations in the case of horizontally curved RC box-girder bridges. This paper investigates the effects of curvature along with abutment contribution on the aforementioned seismic responses at different seismic intensity levels.

There is limited research available concerning the effect of different subtended angles and abutment conditions on the seismic responses of horizontally curved bridges in comparison with equivalent straight bridges. Due to the limited available research in this area, there is no consensus among different seismic design codes on the limitations for subtended curvature angle to analyze a horizontally curved bridge using an equivalent straight bridge. One of the most recent studies conducted in this regard by Siami and Tehrani [35] investigated the limitations recommended by AASHTO specification for using equivalent straight bridges. The results from that study indicated that the boundary conditions of bridges at the place of abutments highly influence the responses of curved bridges compared to those of the equivalent straight bridges. For instance, it was possible to analyze a horizontally curved bridge, having unrestrained (i.e., free) abutment, using an equivalent straight bridge without any limitations for a subtended curvature angle, while for the case of the curved bridges with restrained abutment conditions, the predicted seismic response of the equivalent straight bridges deviated from that of the curved bridges even for the subtended angles that satisfy the code limitations. The effects of abutment properties and seismic intensity levels on the seismic response of equivalent straight bridges have not been studied in the past, and the code provisions need to be re-evaluated considering the influence of these parameters. The current paper contributes to the knowledge on this subject and aims to further investigate the effects of boundary conditions at the place of abutments using a simplified abutment model with different stiffness and strength (i.e., low and high stiffness). In previous research [35], only the seismic responses of the middle columns were investigated in the DBE seismic excitation level, while in the present study, the seismic responses of all bridge columns, including the middle and side columns, and also the seismic displacements at the abutments are evaluated in more detail in local (i.e., radial and tangential) directions for the four-span curved bridges studied. In addition, to investigate the influence of the seismic intensity on the predictions from the equivalent straight bridges, the bridges under study were evaluated at different hazard levels, including the DBE and MCE levels.

2. Bridge Description and Design Procedure

Bridge code specifications promote several linear and nonlinear analyses for design purposes. Although successive design code revisions have improved the seismic performance of bridges [36], in some cases, significant errors still exist. For instance, deviations can occur between the predictions obtained using linear and nonlinear analyses, which are not considered by current code specifications in the design of irregular bridges [5]. Responses of irregular bridges are considerably influenced by higher modes [37, 38]. The AASHTO LRFD bridge

specifications [3] and AASHTO guide specifications [4] state that bridges with subtended angle values of less than 90 degrees and 30 degrees, respectively, under certain conditions (i.e., the bridges that meet some criteria regarding the ratio of span-to-span length and the number of spans) are considered regular and can be analyzed as an equivalent straight bridge. These significantly different limits proposed by these two provisions (i.e., the subtended angles of 90 and 30 degrees) indicate that more research is needed to investigate the influence of different parameters on the maximum limits of the subtended angles in curved bridges. However, Khalafalla and Sennah [39] concluded that these restrictions are not adequately safe to ignore curvature effects. In another research, Siami and Tehrani [35] concluded that abutment models significantly affect the criteria regarding limitations for the subtended angle for using equivalent straight bridges recommended by AASHTO. The current seismic codes do not impose any limitations on the abutment condition of the curved bridges in order to use the equivalent straight bridges.

The case-study bridges in this study have a total length of 160 m, including four spans having equal lengths and symmetric geometry. The deck is a three-celled box-girder with a width of 9.6 m and a depth of 2.4 m. The bridge piers are circular with a diameter of 2.5 m. Since the evaluation of the column diameter and longitudinal reinforcement ratio is out of the scope of this study, regardless of the curvature and irregularity, the design procedure is carried out for the straight bridge model. Column details are tabulated in Table 1. The stiffness and capacity of abutments are not considered in the design to ensure that columns will be able to resist the lateral loads. In the first step of the design process, the bridge is designed according to the force-based specifications of AASHTO [3]. After the preliminary bridge model is created, bridge characteristics should be adjusted to meet the requirements of the seismic design category (SDC) D of AASHTO guide specifications [4]. SDC-D corresponds to structures located in areas expected to experience severe earthquakes but not located close to a major fault. For this purpose, response spectrum analysis (RSA) is carried out using a design response spectrum constructed according to AASHTO [4] recommendations to calculate column bent displacement demands, Δ_D. Then, the pushover analysis is carried out to determine the displacement capacity, Δ_C, of columns. This process continues until displacement capacity demand surpasses displacement ductility demand. The procedure is further demonstrated in Figure 1. The bridges are divided into three categories regarding their abutment modeling assumptions. The first category is described by the bridges without the abutment model (i.e., free abutment). The following two categories contain bridges with lower and higher abutment stiffness. Curved bridges are also characterized as slightly curved (with central curvature angles of 30 and 60 degrees), moderately curved (with central curvature angles of 90 and 120 degrees), and highly curved (with central curvature angles of 150 and 180 degrees). Table 2 represents the notations used for the definition of each bridge model.

Table 1: Middle and side column properties.

Column section	Middle	Side
Section diameter (m)	2.5	2.5
Longitudinal reinforcement bar diameter (mm)	32	32
Longitudinal reinforcement percentage (%)	1.01	1.81
Number of longitudinal bars	62	110
Transverse reinforcement bar diameter (mm)	14	14
Transverse reinforcement percentage (%)	0.5	0.5
Pitch of transverse reinforcement (cm)	5	5

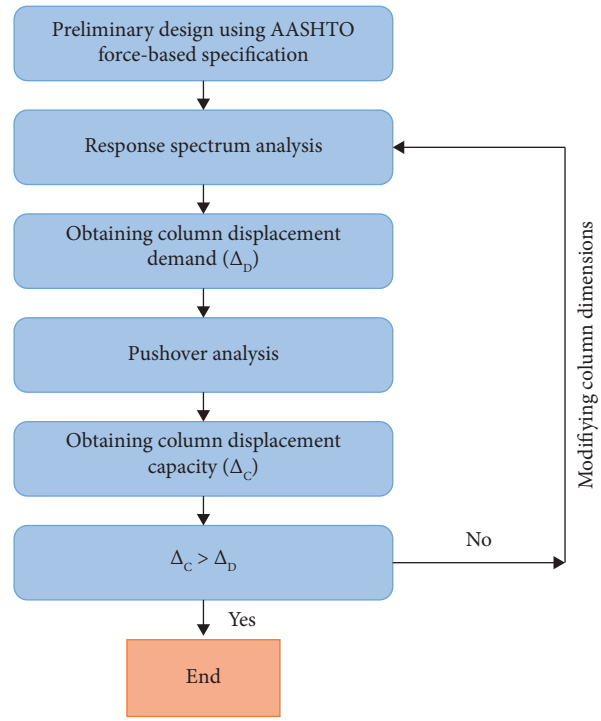

Figure 1: Design flowchart.

3. Numerical Modeling

Three-dimensional finite element bridge models are created in OpenSees [40]. The seismic responses of 21 bridges, including straight and curved configurations with and without the consideration of soil-abutment-bridge interaction, are investigated in this study. The overall dead load of the bridge deck is 156 KN/m. The deck is a prestressed concrete box-girder with no stiffness reduction in the analysis [41], which is assumed to remain elastic during seismic excitations. The deck is modeled as spine lines using elastic beam-column elements at the centroid of its cross section. Pinned connection is used to connect column bents to the superstructure. In the case of single-column bent bridges, a hinged connection results in the cantilever behavior of the column in the transverse direction since no significant rotational restraints are provided at the column top by the superstructure [42]. As presented in Figure 2, a rigid element is defined to account for bent-superstructure overlap with the dimension of 1.3 m., representing the difference between the bottom slab and the vertical centroid of the superstructure cross section above the clear height of the bridge columns.

Table 2: Notations used for the definition of each bridge model.

Central curvature angle (degree)	Abutment typology		
	No abutment (free)	Abutment with lower stiffness (soil + 10 piles)	Abutment with higher stiffness (soil + 20 piles)
Zero (straight)	F0	L0	H0
30	F1	L1	H1
60	F2	L2	H2
90	F3	L3	H3
120	F4	L4	H4
150	F5	L5	H5
180	F6	L6	H6

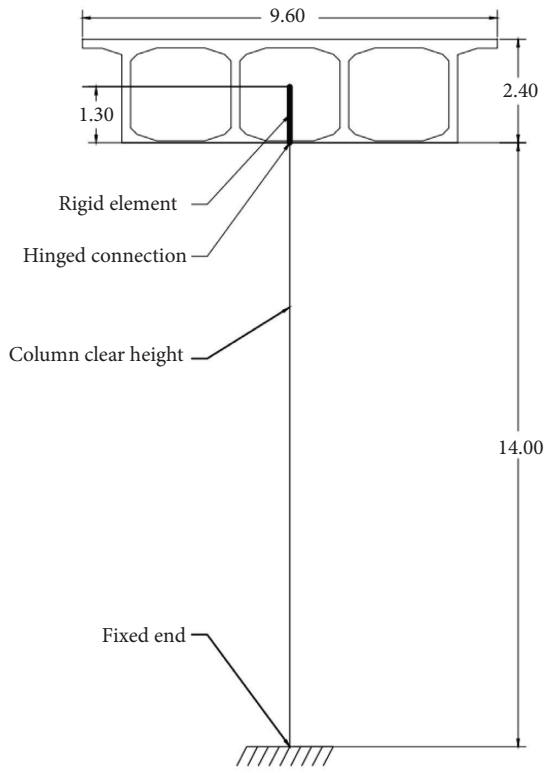

Figure 2: Cross section representing the bent-superstructure joint.

Columns are fixed to the ground to comply with previous research on the seismic response of curved and irregular continuous bridges [5, 35, 43]. It is noted that since this research focuses on the effects of abutment conditions on the seismic response of equivalent straight bridges, consideration of soil-structure-interaction (SSI) at the place of bridge columns is out of the scope of this research, and only the nonlinear behavior at the place of the abutments is considered in the seismic analyses. The influence of SSI at the column foundations on the seismic response of equivalent straight bridges can be the subject of future studies.

3.1. Material Properties. Material properties are assigned following AASHTO recommendations. The confinement provided by transverse reinforcement leads to an increase in the ductility and load-bearing capacity of columns. In this study, the confined concrete is modeled according to the study conducted by Mander et al. [44]. Table 3 presents the characteristics of concrete and reinforcing steel materials. The yield strength of steel rebar (f_y) is 4200 MPa. Nonlinear properties of confined and unconfined concrete are also presented in Table 4, and backbone curves of concrete and steel are depicted in Figure 3.

3.2. Mass Assignment. Superstructure masses are distributed along the longitudinal centerline of the bridge using lumped masses. To achieve an accurate distribution of mass, a sufficient number of nodes and segments should be defined in the OpenSees model. According to the Caltrans recommendation, each bridge span is divided into ten segments [45]. Translational masses are computed according to the equations proposed by Aviram et al. [42]. The mass of each element in the two global directions (i.e., longitudinal and transverse) is calculated based on the dead loads and is assigned at each node, based on its tributary length. Column masses are distributed along the elements. The validity of the mass distribution and accuracy of the restraint application are evaluated by comparing the first four fundamental modal periods obtained using the OpenSees and CSI-Bridge software. As presented in Table 5, the differences obtained from the two software are in an acceptable range.

It is noted that the results from two different software are typically compared to make sure that there are no major errors in modeling, particularly in defining mass and stiffness. Also, the similarity of the results confirms that even using different modeling approaches in different software (e.g., using elastic modeling in CSI-Bridge and nonlinear fiber modeling in OpenSees) results in similar predictions that verify the accuracy of modeling in different methods. In addition to the verification of the predicted modal periods from different software, nonlinear response of the bridge columns will also be verified with the experimental results in Sections 3-4 to validate the accuracy of nonlinear modeling.

3.3. Damping. Previous studies have proposed many modeling methods for Rayleigh damping proportional to the tangential stiffness. Structural responses are greatly influenced in terms of energy damping and the maximum displacement once the damping is applied, either proportional to the primary or tangential stiffness [46–48]. In

Table 3: Material properties.

Materials	Specific weight (KN/m^3)	Poisson ratio	Specific strength (MPa)	Modulus of elasticity (MPa)
Concrete	25	0.2	45	33541
Steel	78.5	0.3	420	200000

Table 4: Nonlinear properties of confined and unconfined concrete.

Concrete types	ε_0	ε_u	f_{pc} (MPa)	f_{pcu} (MPa)
Confined	0.032	0.188	181.6	127.2
Unconfined	0.002	0.005	45.0	0.0

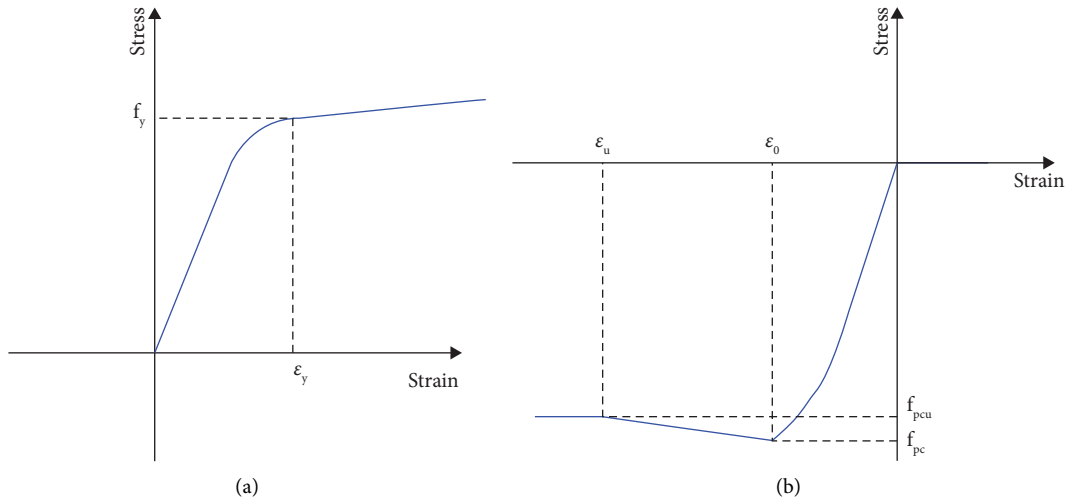

Figure 3: Stress-strain curves of (a) steel and (b) concrete materials.

Table 5: Modal periods (s) obtained from OpenSees and CSI-Bridge software.

Bridge typology	Mode	OpenSees	CSI-Bridge	Difference (%)
Straight	1	1.06	1.07	0.48
	2	0.95	0.92	3.42
	3	0.69	0.72	4.51
	4	0.56	0.56	0.25
Horizontally curved with the subtended angle of 90 degrees	1	1.05	1.06	0.57
	2	0.94	0.90	3.72
	3	0.68	0.71	4.46
	4	0.59	0.60	1.22
Horizontally curved with the subtended angle of 180 degrees	1	1.02	1.03	0.55
	2	0.92	0.87	4.79
	3	0.66	0.69	4.34
	4	0.66	0.68	2.94

the current paper, Rayleigh damping is employed with 5% of critical damping in the first two modes of vibration [42]. As shown in equation (1), a linear combination of the stiffness and mass matrices is used to define the damping matrix [49].

$$[D] = \alpha_0 [M] + \alpha_1 [K], \tag{1}$$

where $[D]$, $[M]$, and $[K]$ are the damping matrix, the mass matrix, and the tangential stiffness matrix, respectively, and α_0 and α_1 are the coefficients of proportionality, which are calculated from the following equation:

$$\begin{cases} \alpha_0 = \dfrac{2\xi\omega_1\omega_2}{(\omega_1 + \omega_2)}, \\ \alpha_1 = \dfrac{2\xi}{(\omega_1 + \omega_2)}. \end{cases} \tag{2}$$

In equation (2), ξ is the damping coefficient of 0.05, ω_1 and ω_2 are the frequencies associated with the first and second modes of vibration, respectively, based on the recommendations by Aviram et al. [42]. The participation of the other modes in the response was not significant for this purpose.

3.4. Column-Bent Modeling. Columns are critical members of concrete bridges that exhibit high fragility [50]. To capture the spread of plasticity and accurate distribution of curvature along column members, fiber sections are assigned to force-based beam-column elements in OpenSees. A sensitivity analysis was conducted on important parameters influencing the seismic responses of bridges. In this regard for the satisfaction of the minimum requirements of seismic code specifications [4, 41], it is decided to use five integration points for force-based beam-column elements, consisting of 20 unconfined concrete fibers, 200 confined concrete fibers and, depending on the longitudinal reinforcement ratio, 62 or 110 reinforcing steel fibers (Figure 4). It should be noted that while force-based elements provide more precise predictions compared to the displacement-based elements in OpenSees, they are prone to nonconvergence problems. To resolve this issue, a code is developed which decreases time steps or changes the algorithm used to solve the nonlinear equations at the iterations that numerical divergence occurs. This method worked very well for this research, although at some analysis steps, it was too time-consuming. Different modeling parameters such as the number of fibers, number of integration points, and analysis time steps were verified by performing a number of sensitivity analyses to ensure the accuracy of the predictions.

Concrete behavior is simulated by Concrete01 material OpenSees [51]. This material is proposed by Kent and Park [52], which defines the monotonic stress-strain curves for confined and unconfined concrete. The behavior of steel bars is modeled by Steel02 material in OpenSees [51], which uses the Menegotto and Pinto [53] model to include isotropic strain hardening. To capture cyclic strength and stiffness degradation in hysteresis loops, MinMax material provided by OpenSees is used [51]. The stress-strain behavior for this material is provided by reinforcing steel material. If the material strain ever exceeds specific threshold values, the material (e.g., Steel02) is assumed to fail. The cyclic behavior of column models is verified with several experimental studies, including the study by Lehman [54], as presented in Figure 5. The P-Δ effects are also accounted for in the analyses.

3.5. Abutment Modeling. Previous studies have suggested various abutment modeling approaches and addressed the issues inherent in abutment modeling [55, 56]. In this study, bridges are modeled either with or without the consideration of soil-abutment-bridge interaction. In all bridge models, the translational vertical direction is restrained at the place of abutments. The abutment model is composed of a rigid element with the length of the superstructure width and five nonlinear springs representing abutment behavior. As presented in Figure 6, the local longitudinal (tangential) response is a function of the gap length, abutment piles, and backfill soil stiffness and strength. As the gap closure occurs, the superstructure collides with the abutment. This impact induces a noticeable amount of inertial force to the abutment. Although the pounding of bridge structures increases the seismic responses of curved bridges and it calls into question the validity of the recommendations from the seismic design provisions for regular curved bridges [2], it is yet outsourced from this study. In order to simulate passive backfill soil response in series with gap elements, elastic-perfectly-plastic-gap (EPPG) material in OpenSees [51] is used. The backbone curve of the EPPG, as presented in Figure 7, is obtained as per equations (3) and (4) [41]. These equations produce a realistic value for embankment fill response based on large-scale tests at UC Davis [57] and UCLA [58].

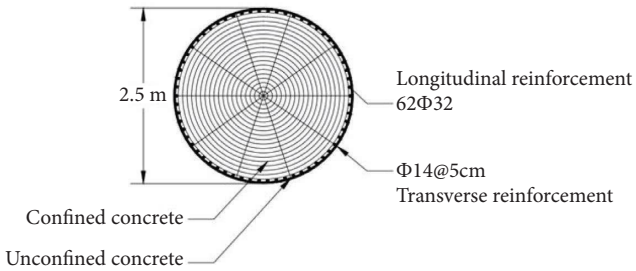

Figure 4: Fiber section simulation of the middle column.

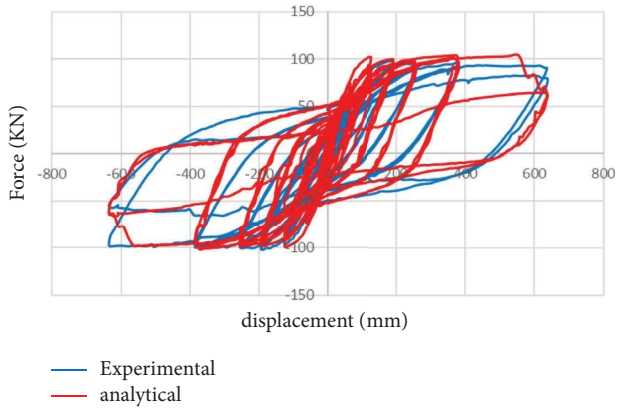

Figure 5: Concrete column behavior validation.

$$K_{\text{abut}} = K_i \times w \times \frac{h}{1.7}, \tag{3}$$

$$P_{bw} = h \times w \times 239\,(kN)\,\frac{h}{1.7}, \tag{4}$$

where w and h denote the width of the back-wall and the abutment height, respectively, and K_{abut} and P_{bw} are the abutment elastic stiffness and ultimate passive capacity of the backfill behind the abutment back wall, respectively. The initial stiffness (K_i) of embankment fill material is assumed to be 14.35kN/mm/m [41]. Probabilistic evaluations have shown that the estimated responses of bridge components are influenced by backfill models in both diaphragm and seat-type abutment bridges [59]. In the local transverse (radial) direction of the abutments, nonlinear springs are used to simulate the abutment pile response. These components also contribute to transferring lateral loads in the longitudinal direction parallel with soil embankment fill. As presented in Figure 8, the response of

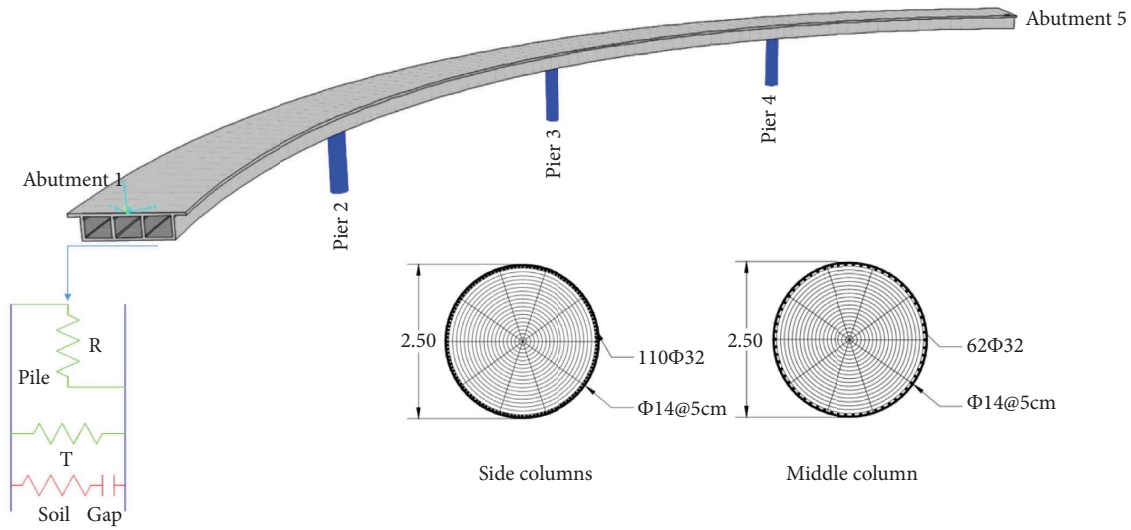

Figure 6: Numerical model of the bridge.

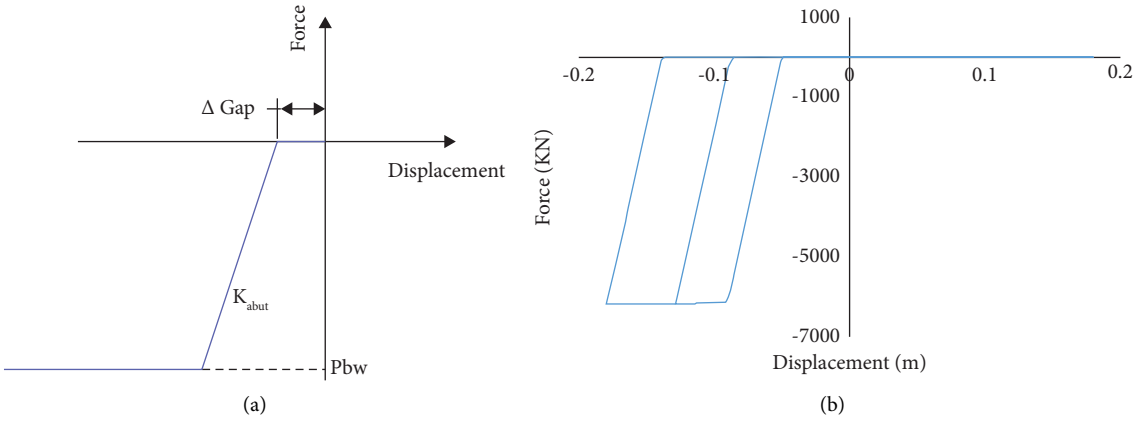

Figure 7: (a) Backbone curve [41] and (b) cyclic behavior of the backfill soil.

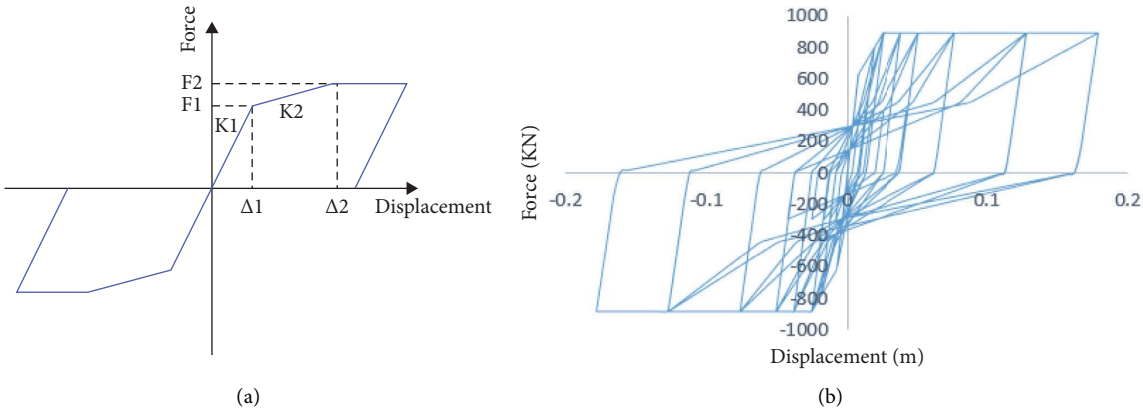

Figure 8: (a) Backbone curve [60] and (b) cyclic behavior of abutment piles.

abutment piles is captured by a trilinear hysteretic model recommended by Choi [60]. This model estimates the stiffness and strength of piles using the empirical pile resistance equation proposed by Goel and Chopra [55], as presented in equations (5) and (6), where R_{pile} and K_{pile} are the ultimate capacity and stiffness of the pile group,

respectively. These equations provide an ultimate strength that is assumed to occur at 1 in. (25 mm) displacement [7, 55].

$$R_{\text{pile}} = 178 \frac{kN}{\text{pile}}, \tag{5}$$

$$K_{\text{pile}} = 7000 \times \frac{kN}{m}. \tag{6}$$

Expansion joints with a length of 5.0 cm along with two different pile configurations (i.e., 10 and 20 piles) are considered to represent abutments with lower and higher stiffness and evaluate the influence of abutment properties on the seismic response of curved bridges. It should be mentioned that the main goal of this paper is to investigate the relative influence of abutment stiffness and strength on the seismic response of equivalent straight bridges, and therefore, more detailed modeling of different abutment components and piles is out of the scope of this research. To further investigate the influence of different abutment modeling techniques on the seismic response, more advanced abutment models can be used in future studies [61]. The previous study on irregular bridges showed that the seismic responses were only slightly improved when piles were added to the abutments in straight bridges [8].

4. Pushover Analysis

To further investigate the effects of abutment modeling on the overall strength of curved bridges compared to straight ones, pushover analysis is carried out in both the longitudinal and transverse directions of the bridge. The chord connecting the abutments represents the longitudinal direction, and the transverse direction is perpendicular to that. Pushover analyses are performed based on a uniform acceleration load pattern. In this approach, nodal forces are applied proportional to the translational mass distribution in the corresponding direction [42]. As presented in Figures 7 to 12, neglecting the contribution of the abutment in the lateral load-resisting system leads to a lower-bound estimate of the longitudinal and transverse resistance of the bridge structures in both straight and horizontally curved configurations. The additional stiffness produced by backfill soil after the gap closure results in a higher strength level of the bridges. Excessive resistance of abutment piles leads to higher initial stiffness and ultimate strength. Doubling the number of piles leads to an increase in the initial stiffness and increases the overall strength of the bridge before the gap closure and ultimate strength after the gap closure. In horizontally curved bridges, soil resistance participates in both longitudinal and transverse directions. The abutment is required to displace 5.0 cm (gap length) in the longitudinal (tangential) direction so that the gap closure occurs and additional soil resistance influences the seismic response. Participation of abutments in seismic response is a crucial factor in the estimation of the overall strength of bridges. For instance, the responses of bridges with free abutments are only slightly influenced by horizontal curvature (as presented in Figures 9–12, the ultimate strength of bridges with straight and horizontally curved geometry having free abutments is merely 10000 KN). However, the effect of horizontal curvature in the overall strength of bridges is more pronounced when the abutment model is considered in analyses.

5. Ground Motion Selection

Type D soil category, with shear wave velocity ranging from 180 m/s to 360 m/s based on the definition of AASHTO [4], is assigned to the bridge site. The considered records are the far-field type with a magnitude from 6.0 to 8.0. The selected ground motions (GMs) comply with the dynamic characteristics of the structure and soil properties of the site, which are obtained from the Pacific Earthquake Engineering Research Center (PEER) GM database (https://ngawest2.berkely.edu). Since far-field records are used in this study, the vertical component of GMs is neglected in the time history analyses. Eleven pairs of GMs are selected out of 200 records and scaled such that the mean SRSS would be compatible with the AASHTO SDC-D design spectrum with a 7 percent probability of exceedance in 75 years, as presented in Figure 13, and the MCE response spectrum, determined by multiplying the design response spectrum by 1.5. During time history analyses, the major component (the one with a larger PGA) is applied to the longitudinal direction, while the minor component is applied to the transverse direction simultaneously. It is noted that no provisions are available in the current codes to explicitly account for the incident angle of the ground motions, and the horizontal components are typically randomly applied in the principal directions [43, 62]. The longitudinal and transverse directions of the curved bridges are considered similar to those defined in Section 4. The GM records are tabulated in Table 6, and Figure 13 represents the spectra of the GMs scaled to be compatible with the design response spectrum in the period range from 0.2 T to 2.0 T, where T is the fundamental period of the bridge. It is noted that the procedure adopted in this research for ground motion scaling is based on the current seismic design codes such as ASCE-07 [63] and AASHTO [3] provisions. It is worth mentioning that there are also some effective methodologies available to incorporate uncertainty in ground motion selection via applying a stochastic excitation [64]. However, the use of such methods is out of the scope of this research and can be investigated in future studies.

6. Results and Discussion

This part consists of a discussion regarding the results obtained from the nonlinear time history analysis of bridge models. The evaluations are made upon the mean responses obtained from the analyses. In this section, local (tangential and radial) seismic demands are evaluated. However, OpenSees software is only capable of providing drift and displacement demands in the global directions. In this

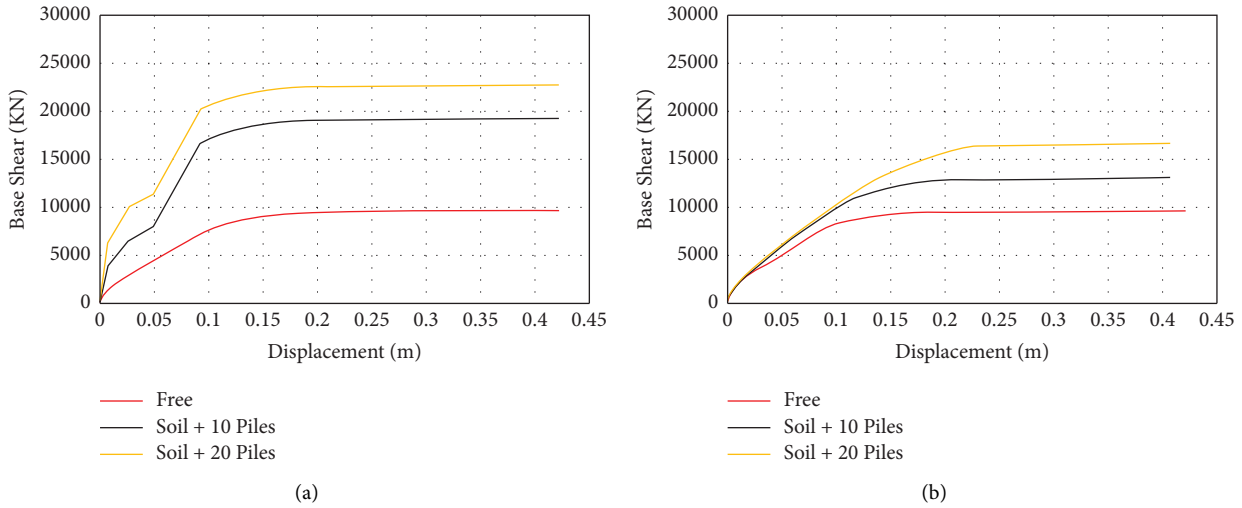

Figure 9: Pushover curves of F0, L0, and H0 bridge models in (a) longitudinal and (b) transverse directions.

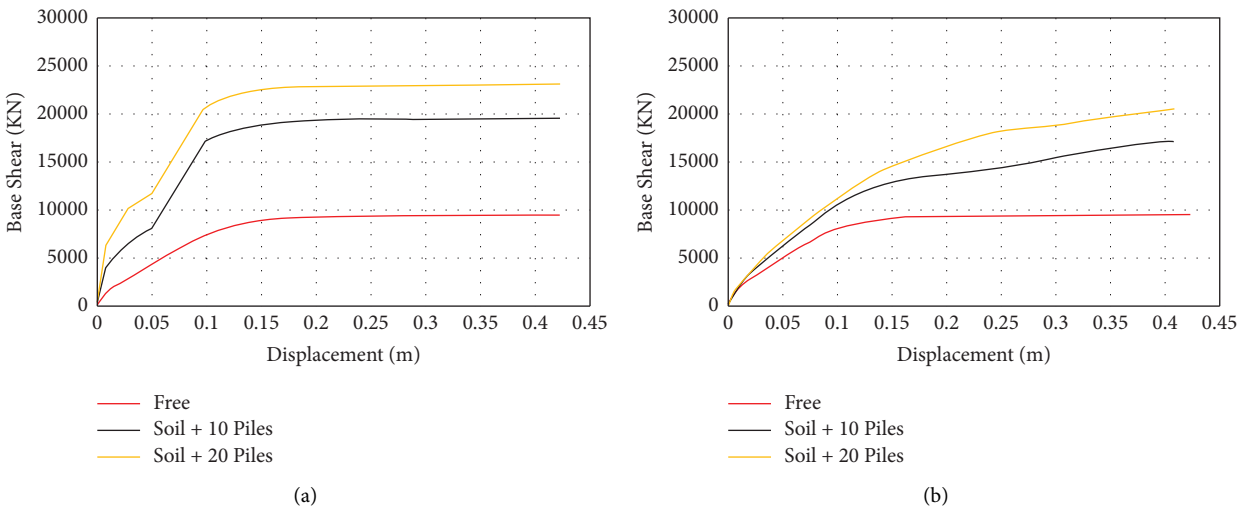

Figure 10: Pushover curves of F1, L1, and H1 bridge models in (a) longitudinal and (b) transverse directions.

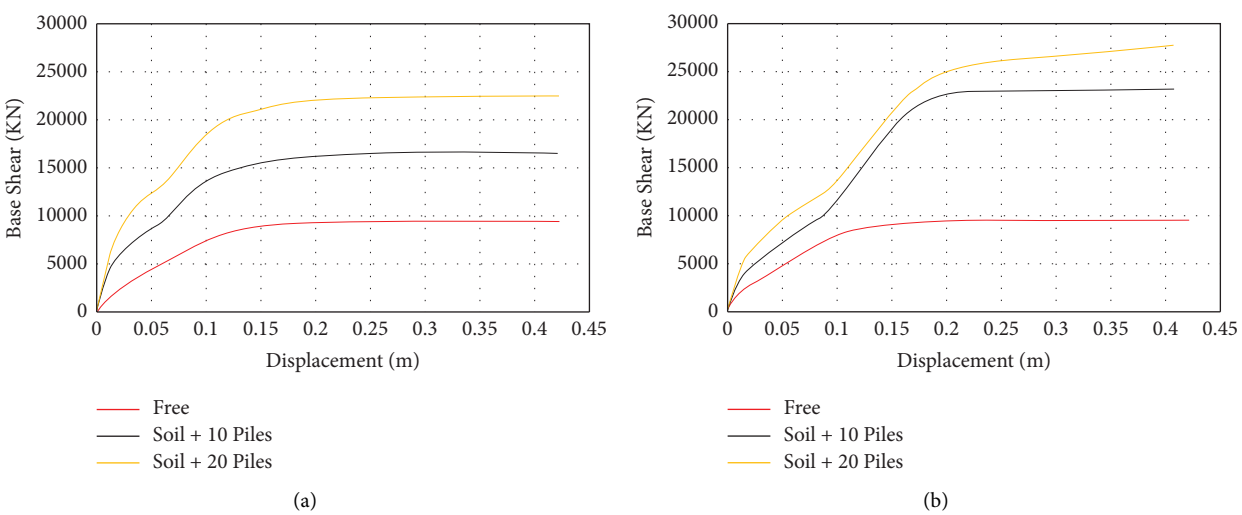

Figure 11: Pushover curves of F3, L3, and H3 bridge models in (a) longitudinal and (b) transverse directions.

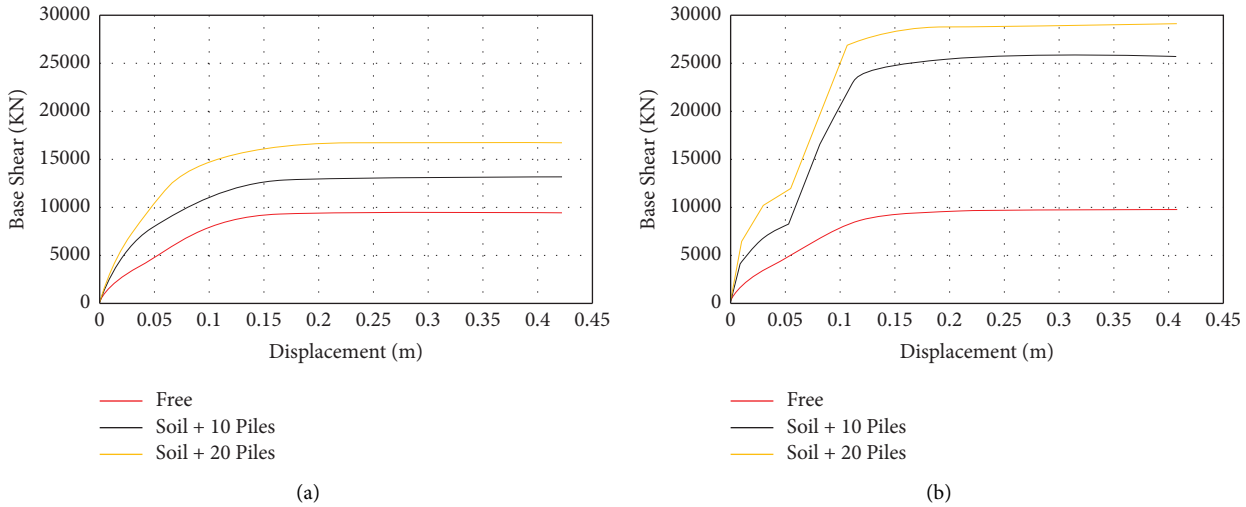

Figure 12: Pushover curves of F6, L6, and H6 bridge models in (a) longitudinal and (b) transverse directions.

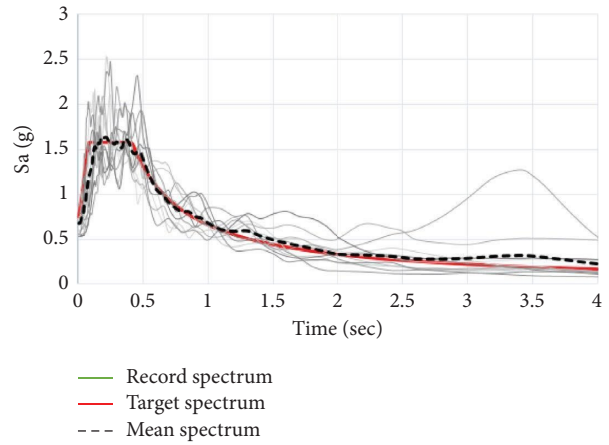

Figure 13: Target design, mean, and record spectra.

Table 6: Description of ground motion records.

#	Name	Year	Station	Magnitude	PGA		Shear wave velocity	Scale factor	
					Major (g)	Minor (g)		DBE	MCE
1	San Fernando	1971	LA-hollywood stor FF	6.61	0.225	0.195	316.46	2.34	3.51
2	Tabas_Iran	1978	Boshruyeh	7.35	0.106	0.085	324.57	3.89	5.84
3	Imperial Valley-06	1979	El centro array #13	6.53	0.139	0.118	249.92	3.66	5.49
4	Superstition Hills-02	1987	Poe road (temp)	6.54	0.475	0.286	193.67	1.40	2.10
5	Loma Prieta	1989	Fremont-Emerson court	6.93	0.192	0.14	284.79	3.15	4.73
6	Manjil_Iran	1990	Abhar	7.37	0.209	0.132	302.64	2.15	3.22
7	Northridge-01	1994	LA-Pico & Sentous	6.69	0.186	0.103	304.68	3.51	5.27
8	Kobe_Japan	1995	Sakai	6.9	0.152	0.127	256.00	2.83	4.25
9	Umbria Marche_Italy	1997	Castelnuovo-Assisi	6.0	0.173	0.105	293.00	3.27	4.91
10	Iwate_Japan	2008	Kitakami Yanagiharach	6.9	0.206	0.154	348.99	3.39	5.09
11	El Mayor-Cucapah_Mexico	2010	RIITO	7.2	0.397	0.376	242.05	1.00	1.50

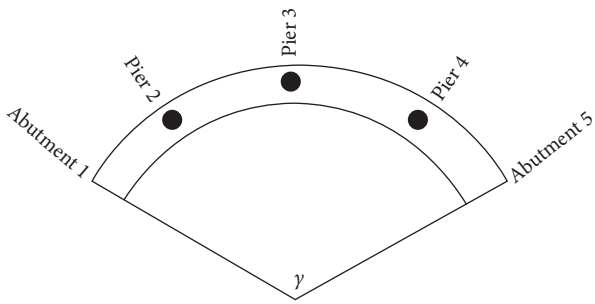

Figure 14: Curvature with a central angle of γ.

Table 7: Guideline for calculating α.

Response	Abutment 1 displacement	Pier 2 drift	Pier 3 drift	Pier 4 drift	Abutment 5 displacement
α	$\gamma/\mathbf{2}$	$\gamma/\mathbf{4}$	$\mathbf{0}$	$-\gamma/\mathbf{4}$	$-\gamma/\mathbf{2}$

regard, global responses are processed at each time step in the analysis using equation (7) to be converted into local demands. Assuming γ as the central curve angle, as presented in Figure 14, α is calculated using Table 7.

$$\begin{bmatrix} T_t \\ A_t \end{bmatrix} = \begin{bmatrix} \cos\alpha & \sin\alpha \\ -\sin\alpha & \cos\alpha \end{bmatrix} \begin{bmatrix} X_t \\ Y_t \end{bmatrix}. \tag{7}$$

In equation (7), X_t, Y_t, T_t, and A_t, respectively, represent the displacement or drift response at the time t during time history analysis in the longitudinal, transverse, tangential, and radial (i.e., azimuthal) directions. Since the structure is symmetrical with respect to its central transverse axis, the seismic responses are determined for the side columns (Pier 2 and Pier 4), and the abutments (Abutment 1 and Abutment 5) are almost equal. In this paper, component responses are based on the drift demands of the middle and side columns (i.e., maximum demand of Piers 2 and 4) and the abutment displacements (i.e., the maximum displacement of Abutments 1 and 5).

The actual maximum vectorial displacement [43, 62] is also defined in this paper as real displacements using equation (8), where R_t is the real response. It is noted that in current computer programs for structural analysis, only the maximum displacements in the global X and Y directions (i.e., X_t and Y_t in equation (8), respectively), corresponding to the longitudinal and transverse directions in this research, are available. However, the actual maximum displacements occur in a different direction (i.e., in a random direction) that does not necessarily correspond to the principal axes of structure. To determine the actual total absolute value of the displacements, also referred to as "real displacement" in this research, a computer code was developed to determine the actual displacement using equation (8) at each analysis time step and predict the maximum actual displacement during the time history analysis.

$$R_t = \sqrt{X_t^2 + Y_t^2}. \tag{8}$$

6.1. Column Drift. According to Figures 15–18, when soil-abutment-bridge interaction is neglected, the superstructure curvature only slightly influences the column drift responses, especially when the seismic excitation level is low. In these models, since the abutments do not participate in the seismic response, the maximum column drift demand is achieved in both tangential and radial directions. As presented in Figures 15 and 18, consideration of the abutments as a part of the lateral load-resisting system in addition to the bridge columns leads to a noticeable decrease in column drift demands in the tangential direction. For the case of straight bridges, the difference in the column drift demands predicted using the F0 and L0 models is almost 55%. The difference increases to 60% once abutments with higher stiffness are used. In the bridge models that the abutment is included in structural modeling, the curved geometry considerably influences the seismic responses in a way that the column drift demands increase in the tangential direction and decrease in the radial direction as the central angle of curvature increases. In this regard, the difference in the predicted column demands using F6 and L6 models is around 30%, and it increases to 50% when the results obtained using the F6 and H6 models are compared in the tangential direction. Adding extra piles to obtain excessive stiffness and resistance has prominent effects on reducing the tangential drift demands. For instance, in the DBE level, a maximum of 20% column drift reduction is observed when abutments with higher stiffness are used compared to the case where abutments with lower participation in load resisting exist. This difference increases up to 25% when responses are evaluated in the MCE excitation level (see Figures 15 and 18). On the other hand, the radial responses are only slightly influenced by extra piles. Regardless of the abutment model used, the middle and side columns of the straight bridges have almost equal displacements in the tangential direction; however, when the soil-abutment-bridge interaction is considered in the structural modeling of horizontally curved bridges, the response of one of the columns becomes more critical. For instance, Pier 2 (i.e., the edge column) in models having abutments with lower stiffness and Pier 3 (i.e., the middle column) in bridges simulated with abutments having higher stiffness are the critical columns, respectively. In fact, the results indicate that a larger horizontal curvature can result in the concentration of seismic demands in a few elements that can eventually lead to significant structural damage. This is similar to the effects of irregularity on the seismic response of bridges with different column heights, as pointed out by Tehrani and Mitchell [8].

On the contrary, in the radial direction, drift demands concerning the middle column are noticeably different from the side columns. As presented in Figure 16, in the straight bridge and the models with a slight curvature, when the abutments are included in the seismic analysis, drift demands of the middle column are higher than or almost equal to the demands of the models without abutment in the DBE and MCE levels, respectively. Previous studies have shown that substructure irregularity leads to an unequal

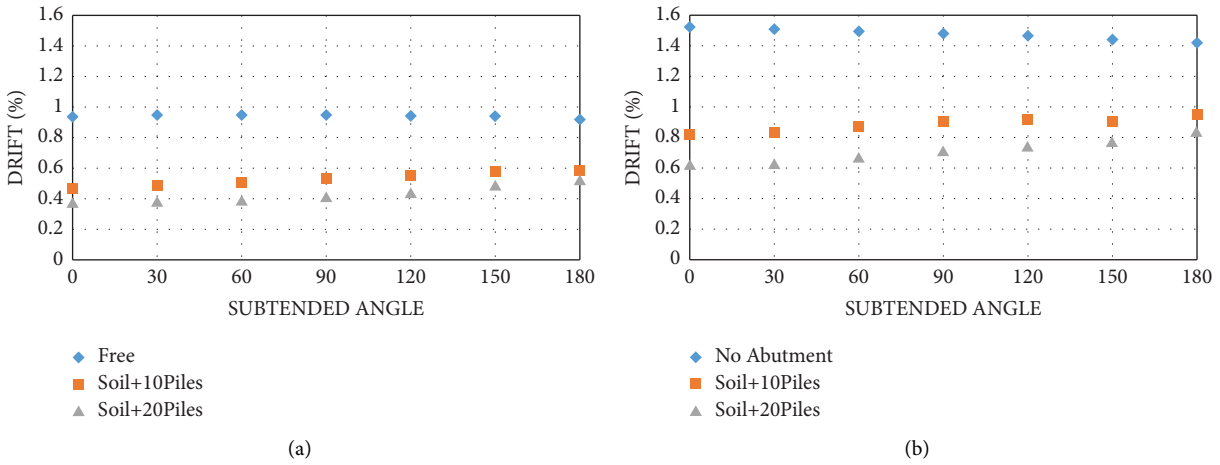

Figure 15: Drift demands of the middle column in all bridge configurations in the tangential direction using GMs compatible to (a) DBE and (b) MCE response spectrums.

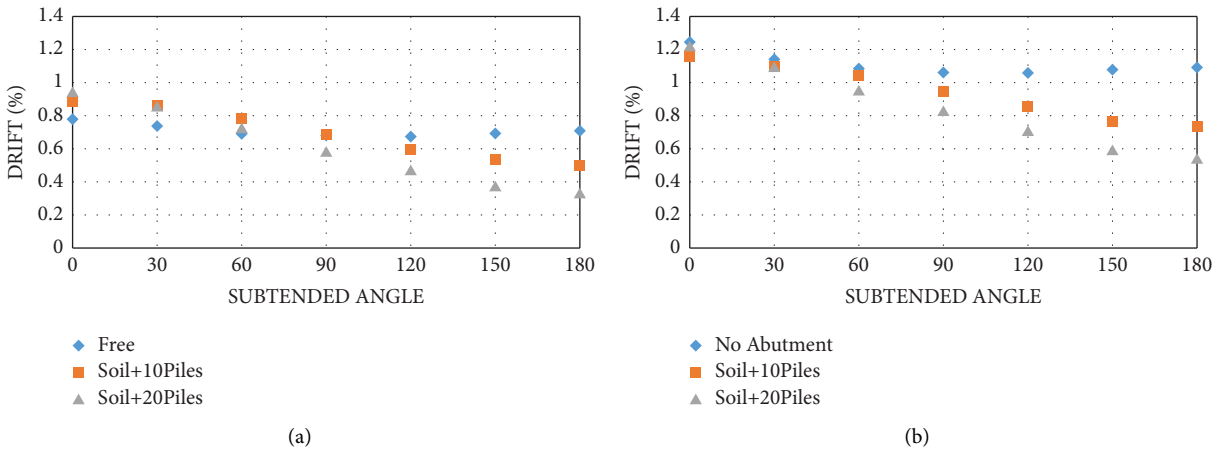

Figure 16: Drift demands of the middle column in all bridge configurations in the radial direction using GMs compatible to (a) DBE and (b) MCE response spectrums.

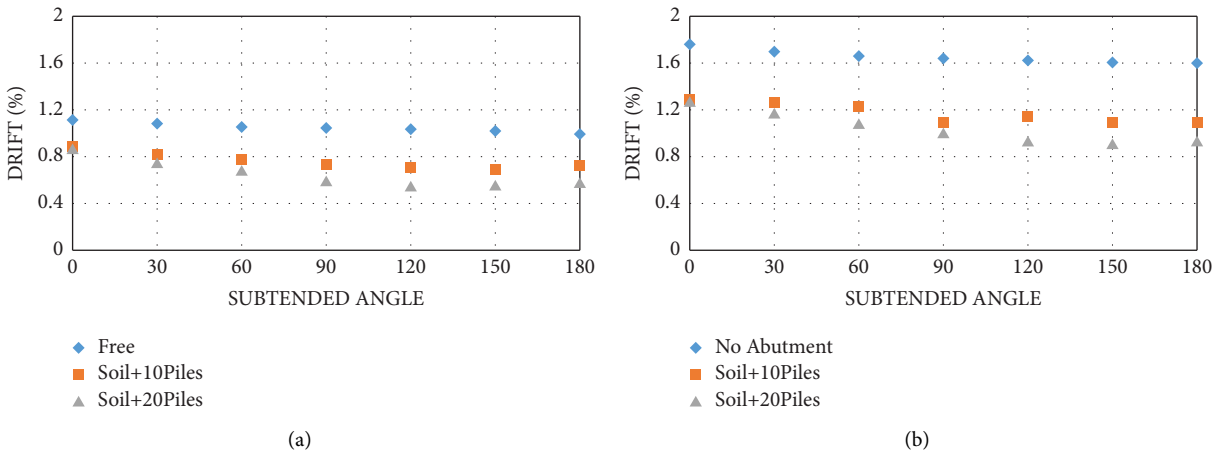

Figure 17: Real drift demands of the middle column in all bridge configurations using GMs compatible to (a) DBE and (b) MCE response spectrums.

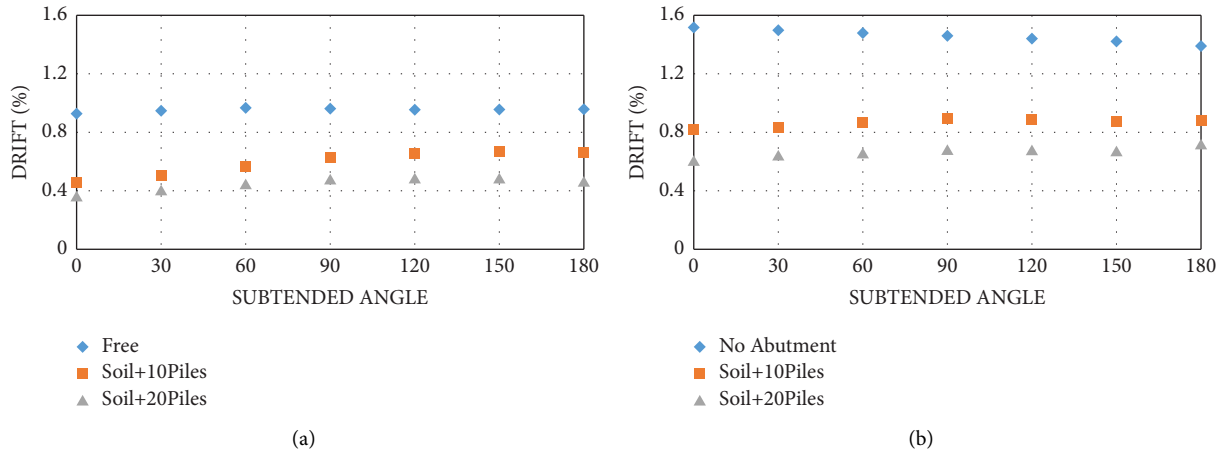

Figure 18: Drift demands of side columns in all bridge configurations in the tangential direction using GMs compatible to (a) DBE and (b) MCE response spectrums.

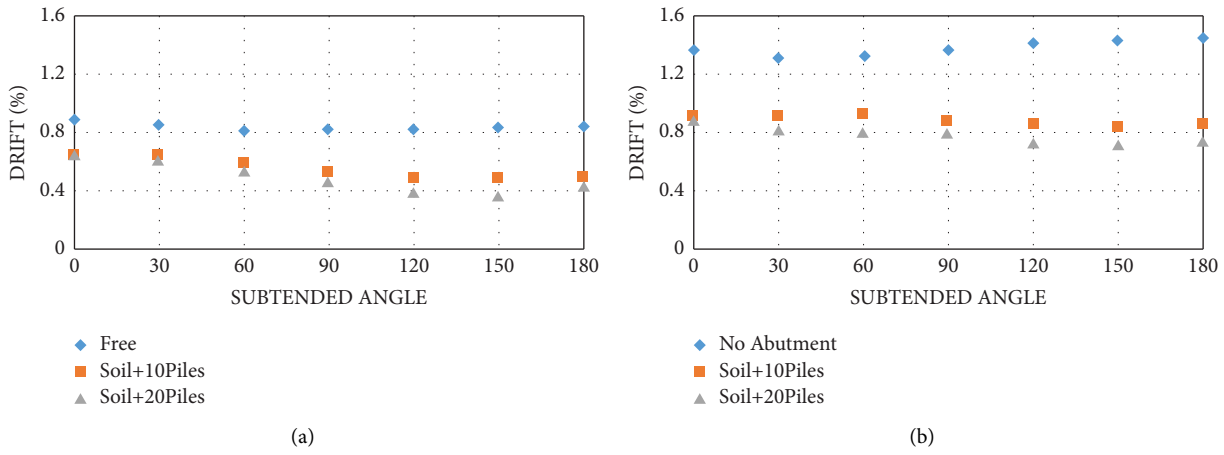

Figure 19: Drift demands of side columns in all bridge configurations in the radial direction using GMs compatible to (a) DBE and (b) MCE response spectrums.

distribution of drift and ductility among columns [5, 7, 35, 65]. Although columns are the same height in this study, the nonuniform dispersion of drift demand is observed when the bridges are restrained by the stiffness and resistance of abutments. Drift demand is almost equally distributed among columns in severely curved bridges in the radial direction. Boundary conditions of abutments do not influence the distribution of displacement demand among middle and side columns in the tangential direction as much as the radial direction. As presented in Figure 19, curvature slightly influences seismic responses of side columns in the radial direction when the records are applied at higher seismic excitation levels.

It is observed from Figure 17 that the real drift responses of the middle column are nearly 15 to 20% larger than drift demands in both perpendicular directions, for all bridge configurations in both seismic excitation levels in the case that free abutment is used. When drift responses are predicted in the tangential direction, this difference increases to 50% in the case that soil-abutment-bridge interaction is accounted for in straight and slightly curved bridges in both seismic excitation levels, and it decreases to almost 10% in highly curved bridges in the DBE level. The difference between real drift demands and responses in the radial direction when the abutment model is included ranges from 5 to 40% in slightly and highly curved models, respectively. Horizontal curvature slightly influences the real seismic displacement demand of the middle column so that the column drifts decrease as the subtended angle increases. However, according to Figure 20, the curvature does not influence the seismic responses of side columns when predicted using real drifts. As presented in Figure 20, the difference between the real and radial drift demands of the side column is around 25% at the DBE level and 20% at the MCE level when the free abutment is used. When soil-abutment-bridge interaction is considered, prediction of the drift demands of straight and slightly curved bridges using real maximum vectorial drifts results in 30% and 5% increase in displacements of side columns in the tangential and radial directions, respectively. Moreover, this difference reaches 20% in highly curved bridge structures in both perpendicular directions.

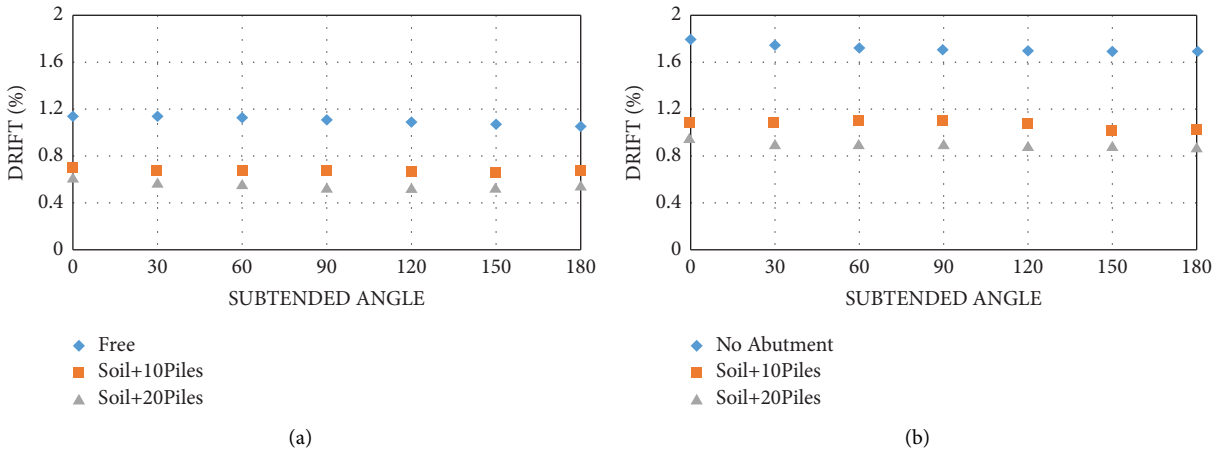

Figure 20: Real drift demands of side columns in all bridge configurations using GMs compatible to (a) DBE and (b) MCE response spectrums.

6.2. Deck Displacement at the Abutment. Lines presented by red color in Figures 21–23 demonstrate the deck displacement at the abutments in straight and horizontally curved bridges having free abutments. Black and yellow colors are representatives of bridges having abutments with low and high stiffness, respectively. Subtended angles are also demonstrated in radar graphs. Comparing the results attributed to bridges with free abutments shows that although curved geometry is not a key factor influencing deck displacements, it leads to a slight increase in deck displacements at the place of abutments in the tangential direction and prevents the deck from excessive displacements in the radial direction. It is revealed from the figures that the consideration of soil-abutment-bridge interaction results in decreasing deck displacement by up to 50% in the tangential direction and 90% in the radial direction in the straight bridge model. By looking through Figures 21 and 22, it is inferred that the addition of backfill soil and abutment piles to the bridge models contributes to the increase and decrease of the deck displacements in the radial and tangential directions, respectively, as the central angle of the curvature increases. For instance, the deck displacement of bridges with no abutments increases by up to 65% (i.e., the difference between the responses of F6 and H6 models) in the tangential direction and decreases by up to 55% (i.e., the difference between the responses of F6 and H6 models) in the radial direction in highly curved bridges, compared to the cases that the abutment response is considered in structural modeling. It is also noted that due to the excessive nonlinear behavior of abutments at the MCE level, the differences of abutment displacements for different subtended angles become smaller. Extra piles are more effective in preventing excessive abutment displacements in the radial direction rather than the tangential direction, particularly when the earthquake records are applied at the MCE level. Large deck displacements at the place of abutments (i.e., displacements larger than the seat width of the abutment in the tangential direction) lead to deck unseating, which is more pronounced in curved bridges due to their excessive deck displacements.

As presented in Figure 22, the real abutment displacements are only slightly influenced by horizontal curvature. When the free abutment is used, the real responses increase about 15% on average compared to the predictions obtained in both perpendicular directions for both seismic excitation levels. As it was observed before, in the case that the abutment model is included, abutment displacements are larger in horizontally curved bridges compared to slightly curved and straight bridges. As a result, the difference between real abutment displacements and the same responses in both perpendicular directions ranges from 75% in straight bridges (L0 and H0 models) to 20% in highly curved bridges (L6 and H6 models).

6.3. Comparison of Seismic Responses of Curved Bridges with an Equivalent Straight Bridge. In this section, seismic responses of curved bridges, including column and deck displacements, are compared with the equivalent straight bridge. Under certain circumstances, AASHTO [3, 4] suggests that the response of curved bridges can be predicted using an equivalent straight bridge model. The equivalent straight bridge is defined to have the same material and section properties as the curved bridge with span lengths equal to the arc lengths of the curved bridge except for the curvature of the superstructure.

As presented in Figure 24, when the abutment model is not included in bridges (i.e., free abutments), the difference between middle and side column displacements of the curved bridges and the equivalent straight bridge in the tangential direction and side column displacement in the radial direction is below 10%. However, this difference for the displacement of the middle column in the radial direction ranges from 10% to 20%. It can be concluded that in the case that the abutment model is neglected, estimating column displacements of curved bridges using an equivalent straight bridge can lead to slightly conservative response predictions, especially in severely and moderately curved bridges.

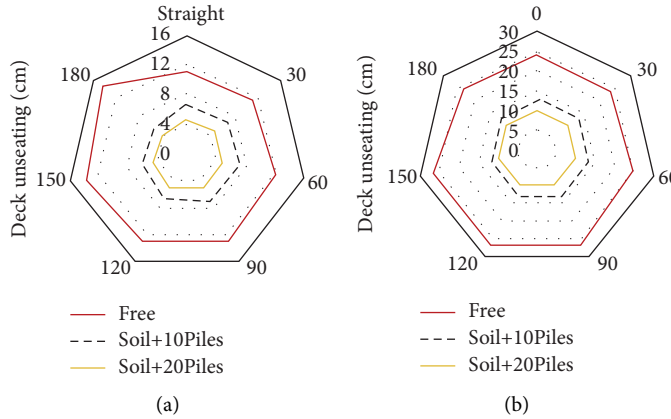

Figure 21: Abutment displacement in all bridge configurations in the tangential direction using GMs compatible to (a) DBE and (b) MCE response spectrums.

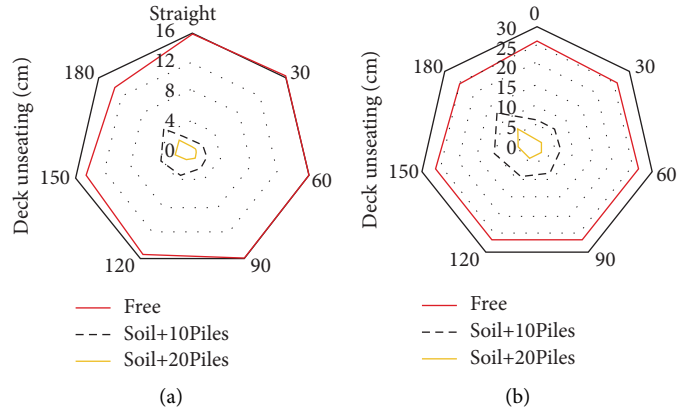

Figure 22: Abutment displacement in all bridge configurations in the radial direction using GMs compatible to (a) DBE and (b) MCE response spectrums.

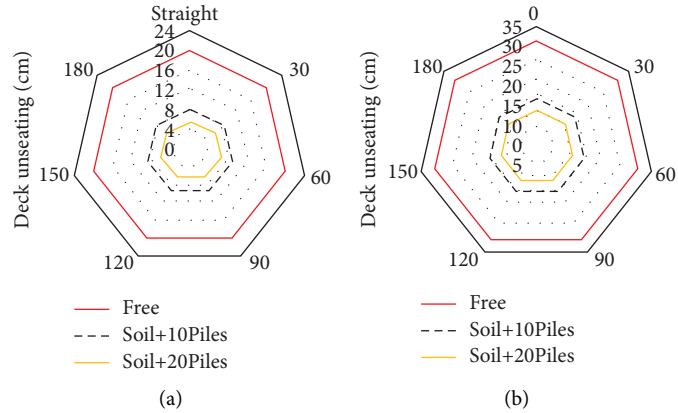

Figure 23: Real abutment displacement in all bridge configurations using GMs compatible to (a) DBE and (b) MCE response spectrums.

According to Figure 24, when abutments with lower stiffness are included in analyses for the highly curved bridges (i.e., bridges with subtended angles higher than 150 degrees), the difference between the column displacements of the curved and equivalent straight bridges ranges from 10% to 40%. This difference ranges from 10% to 60% when abutments with higher stiffness are used. In the horizontally curved bridge with the subtended angle of 30 degrees, the difference of the column responses with respect to the equivalent straight bridge is smaller than 10% in both perpendicular directions. Since a large difference exists between the column demands predicted for the curved

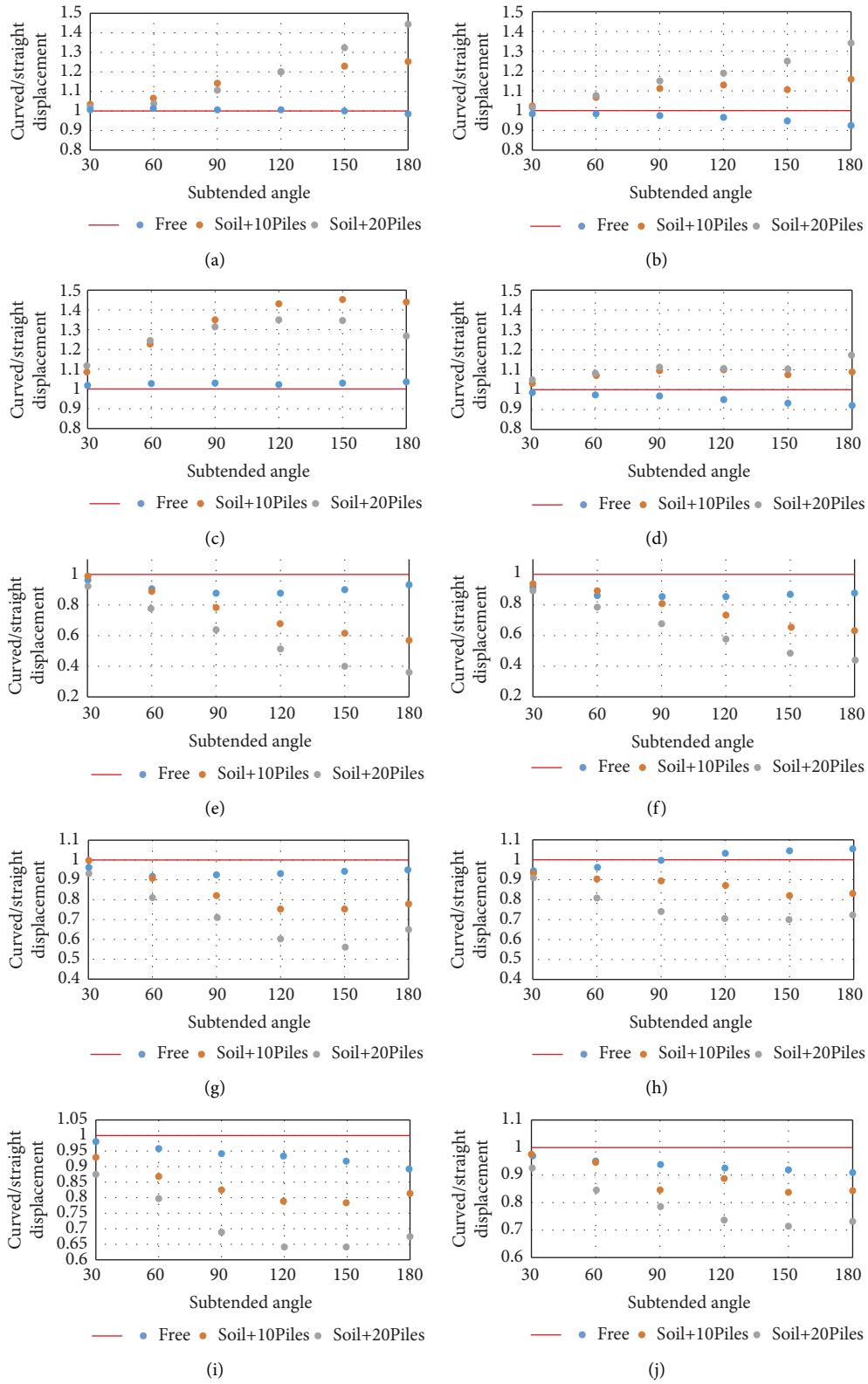

Figure 24: Continued.

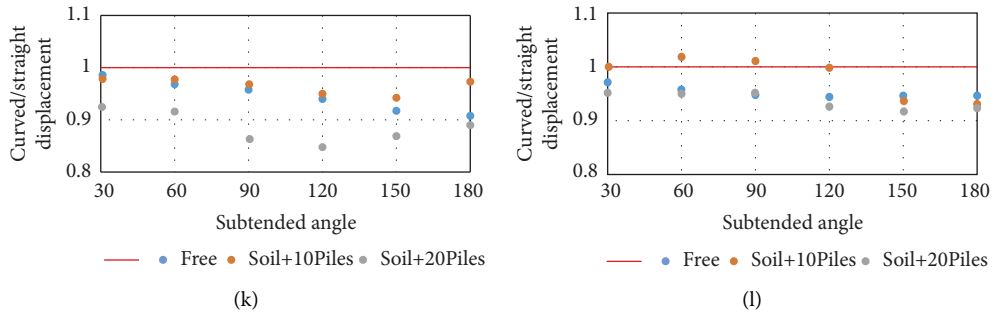

Figure 24: Curved/straight column displacement ratios of the middle column predicted at (a) DBE, (b) MCE levels, side column at (c) DBE, (d) MCE levels in the tangential direction; ratios predicted for middle column at (e) DBE, (f) MCE levels, side column with GMs compatible to (g) DBE, (h) MCE levels in the radial direction, curved/straight real column displacement ratios of the middle column at (i) DBE, (j) MCE levels, side column at (k) DBE, (l) MCE levels.

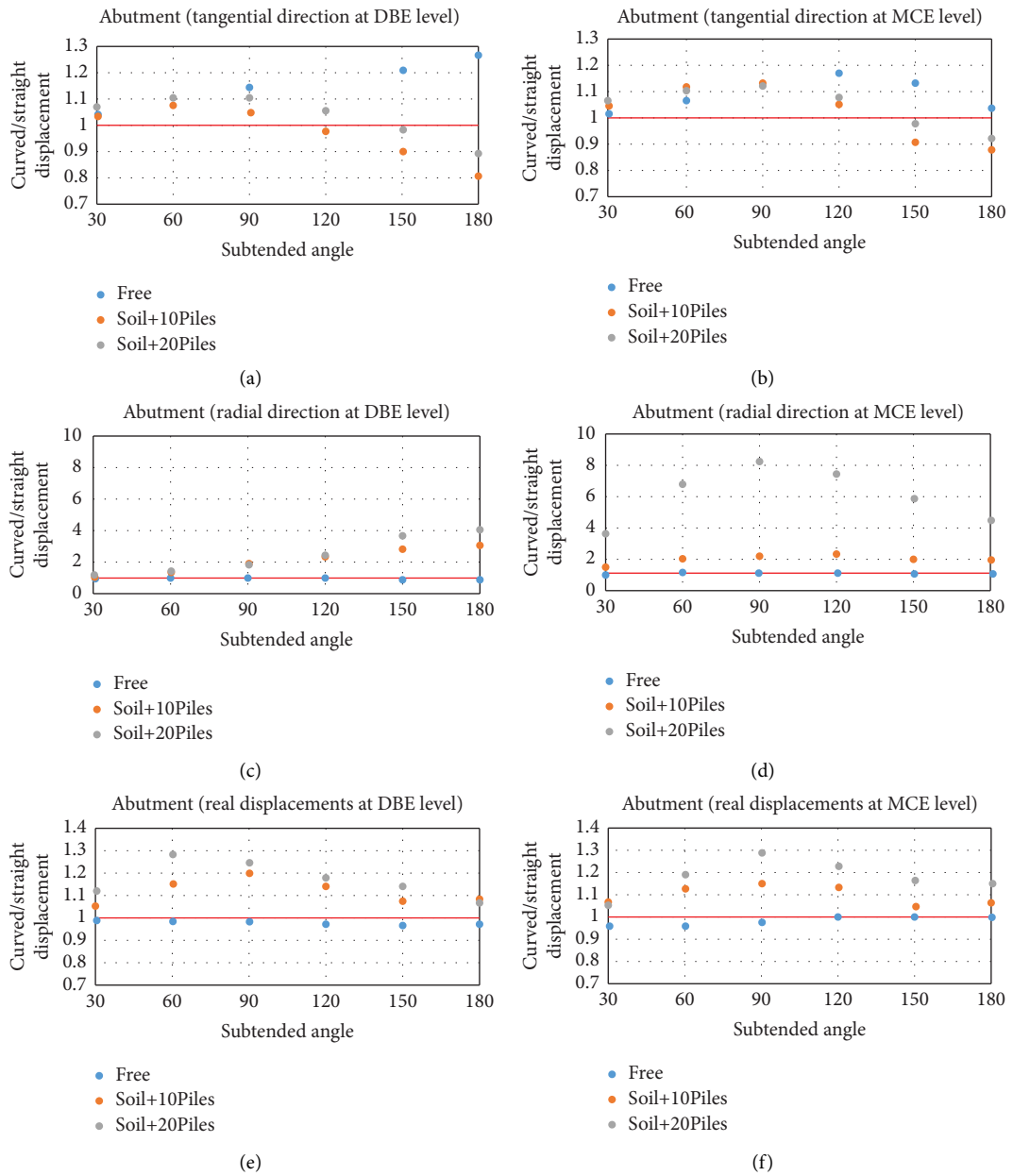

Figure 25: Curved/straight deck displacement ratios at abutments predicted in the tangential direction at (a) DBE, (b) MCE levels; ratios predicted in the radial direction at (c) DBE, (d) MCE levels; ratios predicted using real displacements at (e) DBE, (f) MCE levels.

bridges with respect to the equivalent straight bridge when the abutment is added to bridge models, it is suggested to analyze curved bridges with the subtended angle of higher than 30 degrees using their original shape as recommended by AASHTO [4].

As demonstrated in Figures 21, 22, and 25, nonlinear behavior of the abutments, especially in the MCE excitation level, has made abutments in the curved bridges more involved in seismic load-bearing than columns compared to the straight bridge. As a result, the difference between column displacements of the curved and equivalent straight bridge has decreased at the MCE level.

According to Figures 25(a) and 25(b), when free abutments are used, the difference between the deck displacement at the abutments in the highly and moderately curved bridges and that of the equivalent straight bridge reaches around 20% to 30% in the tangential direction. On the other hand, only a slight difference is observed in the radial direction. Hence, in the assessment of deck displacements at the abutments when soil-abutment-bridge interaction is ignored, it is recommended to use the curved bridge in its original shape rather than estimating responses with an equivalent straight bridge. However, it is noted that this difference in slightly curved bridges (bridges with the subtended angles of 30 and 60 degrees) is negligible. As demonstrated in Figure 25, the existence of the abutment in bridge models significantly increases the difference between the deck displacements of a curved and equivalent straight bridge in the radial direction, especially if responses are evaluated in the MCE excitation level. According to Figure 25(c), in assessing responses of a horizontally curved bridge with a central arch angle of 30 degrees in the DBE level, it is recommended to use an equivalent straight bridge. However, according to Figure 25(d), the displacement of abutments in the radial direction in the curved bridges is around 3.5 times higher than that of the equivalent straight bridge at the MCE excitation level. For larger subtended angles, higher differences are observed. As a result, AASHTO's recommendation is questionable at the MCE level.

In a previous study [35], responses of the middle column were compared to assess the feasibility of using an equivalent straight bridge for the seismic response estimation of a curved bridge at the DBE level. Results obtained in the previous study are validated in the present research by assessing seismic responses of more components, including edge columns and abutments at different local and global coordinates, considering different abutment properties and different hazard levels (i.e., DBE and MCE levels). The results indicate that it is not applicable to predict the seismic displacements of the bridge deck at the abutments in the horizontally curved bridges (even having subtended angles lower than 30 degrees) using an equivalent straight bridge in the MCE level when nonlinear abutment models are included in analysis.

Real response estimates of the horizontally curved bridge and an equivalent straight bridge are also compared in this section. As presented in Figures 24(i) and 24(j), real drift demands of the middle column of the horizontally curved bridges in the models with free abutments have a slight difference from those of the equivalent straight bridge even in the F6 model (the difference is less than 10%). However, when soil-abutment-bridge interaction is considered, this difference increases to 35% and 30% in moderately and highly curved models with the high-stiffness abutments for the DBE and MCE levels, respectively. In the assessment of seismic drift responses, regardless of the abutment modeling assumption, the difference between the real drifts of the side columns in curved bridges and an equivalent straight bridge is less than 10% in the MCE level for all subtended angles (Figure 24(l)). However, this difference in the DBE level in H3, H4, and H5 bridge models exceeds 10% to up to 15% (Figure 24(k)). As presented in Figures 25(e) and 25(f), the difference between the real displacements of the abutment in different subtended angles does not exceed 30% (e.g., in moderately curved bridge models) even in bridges with high-stiffness abutment models.

It is worth mentioning that while in this research, a deterministic approach was adopted for seismic evaluations based on the current seismic practice, more advanced methodologies can be used in future studies to incorporate the uncertainties rooted in bridge/earthquake engineering, such as randomness in material properties, and modeling errors in the seismic evaluations [66].

7. Conclusion

This study investigates the seismic performance of 21 bridge models with straight and horizontally curved configurations using nonlinear time history analyses. For this purpose, eleven sets of ground motion records are scaled and applied to the finite element bridge models created in the OpenSees platform. The bridges are designed and detailed based on the recommendations of AASHTO LRFD bridge design specifications and AASHTO guide specifications. The bridges are divided into three main categories concerning their boundary condition at the place of abutments. To evaluate the influence of abutments on the seismic response of bridges, seat-type abutments with the contribution of backfill soil and two different pile configurations, including 10 piles (i.e., abutments with lower stiffness) and 20 piles (i.e., abutments with higher stiffness) are considered, and the results are compared to the case that soil-abutment-bridge interaction is neglected. Pushover analysis is also carried out on all bridges to obtain their overall strength. The conclusions from this study can be summarized as follows:

(i) Results showed that neglecting soil-abutment-bridge interaction leads to a lower-bound estimate of the strength of the bridge and poses a large error in nonlinear analyses. Backfill soil contributes to seismic responses of horizontally curved bridges in both longitudinal and transverse directions. After the gap closure, the additional stiffness and resistance of backfill soil extremely increase the ultimate strength of the bridge.

(ii) According to the results of nonlinear time history analysis, if the abutments do not participate in the

seismic load-resisting system of the bridge, the superstructure curvature does not significantly influence the column drift responses. By accounting for the soil-abutment-bridge interaction, the drift demands considerably decrease and are noticeably influenced by the bridge curvature. The addition of extra piles to obtain excessive stiffness and resistance has a significant effect on reducing the tangential drift demands; however, it only slightly influences column responses in the radial direction.

(iii) Curved geometry only slightly influences deck displacement responses in bridges with free abutments. However, when the abutment model is included in bridges, horizontal curvature affects deck displacements. In this case, straight bridges have the lowest deck displacements in the radial direction that increase to the highest values in severely curved models. Increasing the number of piles (i.e., increasing the abutment stiffness and strength) not only helps the structure to neutralize the adverse effects of curvature in the longitudinal direction but also contributes to better control the excessive deck displacements in highly curved bridges.

(iv) As the subtended angle increases, curvature slightly affects the responses of bridges with free abutments. However, displacements of the middle column and abutments, especially in the radial direction, are considerably influenced by boundary conditions provided by the abutment model. The difference between the responses of the curved bridges and the equivalent straight bridge also increases in moderate and high curvatures when the abutment model is included. In conclusion, abutment modeling is critically important in the seismic response assessment of curved bridges, and it can significantly change the seismic responses of curved bridges with respect to the equivalent straight bridges.

(v) The results from this study support the findings of the previous study that the seismic responses of the middle columns in horizontally curved bridges with a subtended angle of less than 30 degrees can be evaluated using an equivalent straight bridge. However, the results of this study showed that the deck displacements of moderately and highly curved bridges at both excitation levels in the tangential direction are larger than those of the equivalent straight bridge. The results also indicated that the deck displacements of horizontally curved bridges in the radial direction are significantly larger than the equivalent straight bridge in the MCE excitation level, especially when abutments with higher stiffness are used. The use of the equivalent straight bridges for these cases can result in an underestimation of the superstructure movements of the curved bridge at the abutments that can, in turn, result in unseating of the bridge deck.

(vi) It is found that abutment modeling is critically important in the seismic response assessment of curved bridges compared to straight bridges. However, in current seismic provisions, the effects of seismic intensity, abutment properties, and boundary conditions are not considered, when equivalent straight bridges are used for design. This can result in unsafe designs in some cases. Therefore, the limitation on the subtended angle for analyzing horizontally curved bridges using an equivalent straight bridge is questioned at high seismic intensities (e.g., at the MCE level) based on the results from this study.

Data Availability

Data are available on request from the authors.

Conflicts of Interest

The authors declare that they have no conflicts of interest.

References

[1] D. Linzell, D. Hall, and D. White, "Historical perspective on horizontally curved I girder bridge design in the United States," *Journal of Bridge Engineering*, vol. 9, no. 3, pp. 218–229, 2004.

[2] M. Amjadian and A. K. Agrawal, "Rigid-body motion of horizontally curved bridges subjected to earthquake-induced pounding," *Journal of Bridge Engineering*, vol. 21, no. 12, Article ID 04016090, 2016.

[3] Aashto, *AASHTO LRFD Bridge Design Specifications*, American Association of State Highway and Transportation Officials, Washington, D.C. USA, 2014.

[4] Aashto, *AASHTO Guide Specifications for LRFD Seismic Bridge Design*, American Association of State Highway and Transportation Officials, Washington, D.C, USA, 2011.

[5] M. Sajed and P. Tehrani, "Effects of column and superstructure irregularity on the seismic response of four-span RC bridges," *Structures*, vol. 28, pp. 1400–1412, 2020.

[6] P. Tehrani and D. Mitchell, "Seismic risk assessment of four-span bridges in Montreal designed using the Canadian bridge design code," *Journal of Bridge Engineering*, vol. 19, no. 8, 2014.

[7] P. Tehrani and D. Mitchell, "Effects of column and superstructure stiffness on the seismic response of bridges in the transverse direction," *Canadian Journal of Civil Engineering*, vol. 40, no. 8, pp. 827–839, 2013.

[8] P. Tehrani and D. Mitchell, "Effects of column stiffness irregularity on the seismic response of bridges in the longitudinal direction," *Canadian Journal of Civil Engineering*, vol. 40, no. 8, pp. 815–825, 2013.

[9] K. Karimi-Moridani, P. Zarfam, and M. Ghafory-Ashtiany, "Seismic failure probability of a curved bridge based on analytical and neural network approaches," *Shock and Vibration*, vol. 2017, Article ID 2408234, 18 pages, 2017.

[10] A. Seyedkhoei, R. Akbari, and S. Maalek, "Earthquake-Induced domino-type progressive collapse in regular,

semiregular, and irregular bridges," *Shock and Vibration*, vol. 2019, Article ID 8348596, 18 pages, 2019.

[11] J. Seo, D. G. Linzell, and J. W. Hu, "Nonlinear seismic response analysis of curved and skewed bridge system with spherical bearings," *Advances in Civil Engineering*, vol. 2013, Article ID 248575, 7 pages, 2013.

[12] W. S. Tseng and J. Penzien, "Seismic response of long multiple span highway bridges," *Earthquake Engineering & Structural Dynamics*, vol. 4, no. 1, pp. 25–48, 1975.

[13] D. Williams and W. Godden, "Seismic response of long curved bridge structures: experimental model studies," *Earthquake Engineering & Structural Dynamics*, vol. 7, no. 2, pp. 107–128, 1979.

[14] Q. Han, X. Du, J. Liu, Z. Li, L. Li, and J. Zhao, "Seismic damage of highway bridges during the 2008 Wenchuan earthquake," *Earthquake Engineering and Engineering Vibration*, vol. 8, no. 2, pp. 263–273, 2009.

[15] K. Liu and L. H. Wang, "Earthquake damage of curved highway bridges in 2008 Wenchuan earthquake," in *Advanced Materials Research*, Trans Tech Publ, Stafa-Zurich, Switzerland, 2014.

[16] W.-H. P. Yen, *China Earthquake Reconnaissance Report: Performance of Transportation Structures during the May 12, 2008, M7. 9 Wenchuan Earthquake*, US department of transportation, DC, USA, 2011.

[17] G. C. Lee, *The 512 Wenchuan Earthquake of China–A Preliminary Report*, Powerpoint presentation, Department of Civil, Structural and Environmental Engineering, MCEER, University of Buffalo, NY, USA, 2008.

[18] D. Wang, "Damage to highway bridges during Wenchuan earthquake," *Journal of Earthquake Engineering and Engineering Vibration*, vol. 29, no. 3, pp. 84–94, 2009.

[19] M. Amjadian and A. K. Agrawal, "Dynamic characteristics of horizontally curved bridges," *Journal of Vibration and Control*, vol. 24, no. 19, pp. 4465–4483, 2018.

[20] J. Wieser, "A methodology for the experimental evaluation of seismic pounding at seat-type abutments of horizontally curved bridges," *Structures Congress*, 2012.

[21] E. Amirihormozaki, G. Pekcan, and A. Itani, "Analytical fragility functions for horizontally curved steel I-girder highway bridges," *Earthquake Spectra*, vol. 31, no. 4, pp. 2235–2254, 2015.

[22] D. G. Linzell and V. P. Nadakuditi, "Parameters influencing seismic response of horizontally curved, steel, I-girder bridges," *Steel and Composite Structures*, vol. 11, no. 1, pp. 21–38, 2011.

[23] H. Wu and W. S. Najjar, "Parametric seismic analysis of curved steel box-girder bridges with two continuous spans," *Bridge Structures*, vol. 3, no. 3-4, pp. 205–213, 2007.

[24] M. N. Abdel-Salam and C. P. Heins, "Seismic response of curved steel box girder bridges," *Journal of Structural Engineering*, vol. 114, no. 12, pp. 2790–2800, 1988.

[25] M. Minavand and M. G. Ashtiany, "Seismic evaluation of horizontally curved bridges subjected to near-field ground motions," *Latin American Journal of Solids and Structures*, vol. 16, no. 2, 2019.

[26] H. Pahlavan, B. Zakeri, G. G. Amiri, and M. Shaianfar, "Probabilistic vulnerability assessment of horizontally curved multiframe RC box-girder highway bridges," *Journal of Performance of Constructed Facilities*, vol. 30, no. 3, Article ID 04015038, 2016.

[27] J.-S. Jeon, R. DesRoches, T. Kim, and E. Choi, "Geometric parameters affecting seismic fragilities of curved multi-frame concrete box-girder bridges with integral abutments," *Engineering Structures*, vol. 122, pp. 121–143, 2016.

[28] R. S. Shirazi, G. Pekcan, and A. Itani, "Analytical fragility curves for a class of horizontally curved box-girder bridges," *Journal of Earthquake Engineering*, vol. 22, no. 5, pp. 881–901, 2018.

[29] S. Mangalathu, E. Choi, H. C. Park, and J. S. Jeon, "Probabilistic seismic vulnerability assessment of tall horizontally curved concrete bridges in California," *Journal of Performance of Constructed Facilities*, vol. 32, no. 6, Article ID 04018080, 2018.

[30] N. Serdar and R. Folić, "Vulnerability and optimal probabilistic seismic demand model for curved and skewed RC bridges," *Engineering Structures*, vol. 176, pp. 411–425, 2018.

[31] Z. Tang, H. Ma, J. Guo, and Z. Li, "Effect of soil-structure interaction on seismic performance of long-span bridge tested by dynamic substructuring method," *Shock and Vibration*, vol. 2017, Article ID 4358081, 12 pages, 2017.

[32] I. P. Lam and G. R. Martin, "Seismic design for highway bridge foundations," in *Lifeline Earthquake Engineering: Performance, Design and Construction*, ASCE, Canada, 1986.

[33] S. A. Mitoulis, "Seismic design of bridges with the participation of seat-type abutments," *Engineering Structures*, vol. 44, pp. 222–233, 2012.

[34] G. Fiorentino, C. Cengiz, F. De Luca et al., "Integral abutment bridges: investigation of seismic soil-structure interaction effects by shaking table testing," *Earthquake Engineering & Structural Dynamics*, vol. 50, no. 6, pp. 1517–1538, 2021.

[35] R. K. Siami and P. Tehrani, "Investigating seismic behavior of horizontally curved RC bridges with different types of irregularity in comparison with equivalent straight bridges," *Structures*, vol. 33, pp. 2570–2586, 2021.

[36] S. Shekhar, J. Ghosh, and S. Ghosh, "Impact of design code evolution on failure mechanism and seismic fragility of highway bridge piers," *Journal of Bridge Engineering*, vol. 25, no. 2, Article ID 04019140, 2020.

[37] S. Maalek, R. Akbari, and M. R. Maheri, "The effect of higher modes on the regularity of single-column-bent highway viaducts," *Bridge Structures*, vol. 5, no. 1, pp. 29–43, 2009.

[38] E. Aboutorabian and M. Raissi Dehkordi, "New extended quantitative local and global regularity index for single-and multiframe RC bridges based on modal vector correlation," *Shock and Vibration*, vol. 2021, Article ID 6860335, 17 pages, 2021.

[39] b. I. E. Khalafalla and K. Sennah, "Curvature limitations for concrete box-girder and solid-slab bridges," *ACI Structural Journal*, vol. 111, no. 5, p. 1003, 2014.

[40] F. McKenna, G. L. Fenves, and M. H. Scott, *Open System for Earthquake Engineering Simulation*, Opensees, CA, USA, 2000.

[41] C. Caltrans, *Seismic Design Criteria (SDC), V 2.0*, California Department of Transportation, Sacramento, CA, 2019.

[42] A. Aviram, K. R. Mackie, and B. Stojadinovic, *Guidelines for Nonlinear Analysis of Bridge Structures in California*, Technical Reports, National Technical Reports Library, USA, 2008.

[43] P. Tehrani and R. Ghanbari, "Investigating different methods for application of earthquake records in seismic evaluation of irregular RC bridges considering incident angles," *Structures*, vol. 32, pp. 1717–1733, 2021.

[44] J. B. Mander, M. J. N. Priestley, and R. Park, "Theoretical stress-strain model for confined concrete," *Journal of Structural Engineering*, vol. 114, no. 8, pp. 1804–1826, 1988.

[45] P. Kaviani, F. Zareian, and E. Taciroglu, "Seismic behavior of reinforced concrete bridges with skew-angled seat-type abutments," *Engineering Structures*, vol. 45, pp. 137–150, 2012.

[46] M. Abbasi and M. A. Moustafa, "Effect of viscous damping modeling characteristics on seismic response of bridges," in *Proceedings of the 2th Istanbul Bridge Conference*, Sheraton Istanbul, August 2016.

[47] A. Chopra and F. Mckenna, "Modeling viscous damping in nonlinear response history analysis of buildings," in *Proceedings of the 16th World Conference on Earthquake Engineering*, Santiago, Chile, February 2017.

[48] L. Petrini, C. Maggi, M. J. N. Priestley, and G. M. Calvi, "Experimental verification of viscous damping modeling for inelastic time history analyzes," *Journal of Earthquake Engineering*, vol. 12, no. sup1, pp. 125–145, 2008.

[49] R. Clough and J. Penzien, *Of Structures*, McGraw-Hill, NY, USA, 1975.

[50] T. Wu, Z. Li, and S. Liu, "Elaborate modeling and fragility assessment of a multiframe PC box-girder bridge with intermediate hinges in California," *Shock and Vibration*, vol. 2021, Article ID 6046209, 18 pages, 2021.

[51] S. Mazzoni, *OpenSees Command Language Manual. Pacific Earthquake Engineering Research*, p. 264, PEER Center, TN, India, 2006.

[52] D. C. Kent and R. Park, "Flexural members with confined concrete," *Journal of the Structural Division*, vol. 97, no. 7, pp. 1969–1990, 1971.

[53] M. Menegotto and P. Pinto, "Method of analysis for cyclically loaded reinforced concrete frames including changes in geometry and non-elastic behavior of elements under combined normal forces and bending moment," *IASBE Proceedings*, 1973.

[54] D. E. Lehman, *Seismic Performance of Well-Confined concrete Bridge Columns*, University of California, Berkeley, 1998.

[55] R. K. Goel and A. K. Chopra, "Evaluation of bridge abutment capacity and stiffness during earthquakes," *Earthquake Spectra*, vol. 13, no. 1, pp. 1–23, 1997.

[56] A. Aviram, K. R. Mackie, and B. Stojadinovic, "Effect of abutment modeling on the seismic response of bridge structures," *Earthquake Engineering and Engineering Vibration*, vol. 7, no. 4, pp. 395–402, 2008.

[57] B. H. Maroney and Y. H. Chai, "Bridge abutment stiffness and strength under earthquake loadings," in *Proceedings of the 2nd International Workshop on the Seismic Design of Bridges*, NY, USA, June 1994.

[58] J. P. Stewart, *Full Scale Cyclic Testing of Foundation Support Systems for Highway Bridges. Part II: Abutment Backwalls*, 2007.

[59] Y. Xie, Q. Zheng, C. S. W. Yang et al., "Probabilistic models of abutment backfills for regional seismic assessment of highway bridges in California," *Engineering Structures*, vol. 180, pp. 452–467, 2019.

[60] E. Choi, *Seismic Analysis and Retrofit of Mid-America Bridges*, Georgia Institute of Technology, Atlanta, GA, 2002.

[61] P. Tehrani and T. Alizadeh, "Effect of different abutment modeling strategies on the seismic response of irregular reinforced concrete bridges," *International Journal of Civil Engineering*, 2022.

[62] P. Tehrani and D. Mitchell, "Prediction of mean responses of RC bridges considering the incident angle of ground motions and displacement directions," *Applied Sciences*, vol. 11, no. 6, p. 2462, 2021.

[63] Asce, *Minimum Design Loads and Associated Criteria for Buildings and Other Structures*, American Society of Civil Engineers, Virgina, USA, 2017.

[64] A. Abdollahi, A. Amini, and M. A. Hariri-Ardebili, "An uncertainty-aware dynamic shape optimization framework: gravity dam design," *Reliability Engineering & System Safety*, vol. 222, Article ID 108402, 2022.

[65] S. Soltanieh, M. M. Memarpour, and F. Kilanehei, "Performance assessment of bridge-soil-foundation system with irregular configuration considering ground motion directionality effects," *Soil Dynamics and Earthquake Engineering*, vol. 118, pp. 19–34, 2019.

[66] M. Kia, A. Amini, M. Bayat, and P. Ziehl, "Probabilistic seismic demand analysis of structures using reliability approaches," *Journal of Earthquake and Tsunami*, vol. 15, no. 03, Article ID 2150011, 2021.